Check for updates

Improvement of the CIGS solar cell performance: structure based on a ZnS buffer layer

Souad Tobbeche[1] · Salim Kalache[1] · Mourad Elbar[1] · Mohamed Nadjib Kateb[1] · Mohamed Redha Serdouk[1]

Abstract

Cu(In,Ga)Se$_2$ (CIGS) based thin film solar cells are the most efficient thin-film solar cells today. The non-toxic and wide band-gap zinc sulphide (ZnS) is a promising material to replace the cadmium sulfide (CdS) as the buffer layer in CIGS based solar cells. In this work we present a simulation study of a CIGS based solar cell with a buffer layer of ZnS, using the simulator Silvaco-Atlas. Our primary simulation shows a 22.6% efficiency of the CIGS solar cell with the CdS buffer layer which is comparable to reported and highest experimental results. However, the simulated efficiency of the CIGS solar cell with the ZnS buffer layer as high as 23.54% was achieved. The effects of layer parameters like the thickness, the acceptor and donor densities of the CIGS absorber and ZnS buffer layers and the CBO on the photovoltaic parameters of the ZnS/CIGS solar cell are optimized in order to improve the performance of the ZnS/CIGS solar cell. The highest efficiency of 27.33% is achieved when the ZnS buffer and the CIGS absorber layers have thicknesses of 0.025 μm and 4 μm with acceptor and donor densities of 6×10^{17} cm^{-3} and 10^{18} cm^{-3}, respectively and a CBO in the range -0.05 to 0.05 eV. The present results of simulation can help the development of the solar cells with higher conversion efficiency and low cost.

Keywords CIGS thin film solar cell · ZnS buffer layer · Simulation · Optimization · Silvaco-Atlas

1 Introduction

Thin film solar cells based on chalcopyrite Cu(In$_{1-x}$Ga$_x$)Se$_2$ (CIGS) semiconductor material have received a lot of attention recently due to their low production cost, excellent conversion efficiency and stability. The compound semiconductor CIGS exhibits interesting properties such as a direct tunable band-gap energy in the range 1.04–1.68 eV to exploit the greatest solar irradiance and a high absorption coefficient of ~10^5 cm^{-1} in the visible range

✉ Souad Tobbeche
  s.tobbeche@univ-biskra.dz

[1] Laboratoire des Matériaux Semiconducteurs et Métalliques (LMSM), Département de Génie-Electrique, Faculté des Sciences et de la Technologie, Université de Biskra, BP 145, 07000 Biskra, Algeria

of the solar spectrum. Solar cells based on CIGS absorbers and CdS buffer layers are among the most promising thin-film photovoltaic technologies with a record of conversion efficiency reaching 22.6% (Jackson et al. 2016) achieved by the ZSW (Zentrumfür Sonnenenergie and Wasserstoff Forschung—Germany) center at AM 1.5G solar spectrum. The high efficiency CIGS solar cells have been grown in the conventional configuration composed of a thin CdS buffer layer deposited onto a CIGS absorber layer with a highly resistive undoped zinc oxide (i-ZnO) layer introduced between the CdS and Al-doped ZnO (ZnO:Al) to carry the current. The CdS band-gap energy of about 2.4–2.5 eV is non-optimal for the solar cell performance due to the optical absorption losses from the CdS buffer layer especially in the short wavelength range (Hariskos et al. 2005; Siebentritt 2004). Moreover, the CdS buffer layer can give rise to health and environmental safety due to the toxic cadmium (Cd) containing waste generated during the deposition process. Therefore, many research groups in the realm of CIGS solar cells have focused on the development of alternative materials for a Cd-free buffer layer in CIGS solar cells. Several nontoxic low-absorbing transparent oxide semiconductors have been investigated. Zn(S,O,OH)/CIGS, $Zn_{1-x}Sn_xO_y$/CIGS, In_xS_y/CIGS and $Zn_xMg_{1-x}O$/CIGS cells could attain high conversion efficiencies of 21.0% (Friedlmeier et al. 2015), 18.2% (Lindahl et al. 2013), 18.2% (Spiering et al. 2016) and 18.1% (Törndahl et al. 2010), respectively. Zinc sulfide ZnS is an interesting material with a band-gap energy of ~ 3.8 eV which is much larger than that of CdS. Hence, the ZnS buffer layer of CIGS solar cells is expected to improve the solar cell current generation at the shorter wavelengths. The achieved efficiencies of CIGS solar cells with ZnS buffer layers are comparable to those obtained for CIGS solar cells made from CdS buffer layers (Friedlmeier et al. 2015; Nakamura et al. 2013; Martin Green et al. 2016).

Along with the experimental work, the solar cell simulation has become indispensable tool for analyzing the performance and optimizing the design of any kind of efficient solar cells. The performance of CIGS solar cells with different buffer layers such as CdS, ZnO, ZnS(O,H), ZnSe, InS and $Zn_{1-x}Mg_xO$ has been studied by simulation (Khoshsirat et al. 2015; Chelvanathan et al. 2010; Mostefaoui et al. 2015; Movla 2014; Asaduzzaman et al. 2017b; Za'Abar et al. 2018), and ZnS/CIGS solar cells have been reported as promising structures compared to CdS/CIGS solar cells (Mostefaoui et al. 2015; Asaduzzaman et al. 2017b). There were several numerical studies showing the improvement of the performance of the ZnS/CIGS solar cell with the important parameters of ZnS/CIGS cells such as, the thickness, band gap and gradient band gap of the CIGS absorber layer, thickness of the ZnS buffer layer, acceptor and donor concentrations of absorber and buffer layers and conduction band offset (CBO) (Luo et al. 2017; Asaduzzaman et al. 2017b; Sylla et al. 2017; Park and Shin 2018). The optimization of the buffer and the absorber layers' thicknesses for a ZnS/CIGS solar cell using ADEPT 2.1 software leads to an optimum efficiency of 24.62% (Hosen et al. 2017; Asaduzzaman et al. 2017b). The Performance of ZnS/CIGS solar cells at various parameters, in particular the thickness and Ga-content of the absorber layer, thickness of the buffer layer and acceptor and donor concentrations of absorber and buffer layers were numerically studied using AFORS-HET simulator leads to a maximum conversion efficiency of 26% (Sylla et al. 2017). The simulation results suggest that it is possible to achieve a 26.3% conversion efficiency in the ZnS/CIGS solar cell with optimized ZnS and CIGS physical properties such as the electron affinity of the ZnS layer, the thickness of the ZnS layer, the acceptor concentration and the thickness of the CIGS layer using SCAPS simulator (Fridolin et al. 2018).

In this work, we performed the numerical simulation to study CdS/CIGS and ZnS/CIGS solar cells. The two dimensional Silvaco-Atlas software (Atlas User's Manual device simulation software 2013) is used for simulating the solar cells and photovoltaic parameters of

the simulated solar cells have been calculated. Firstly, we reported the modelling and simulation results of a CdS/CIGS based solar cell which are validated by comparing them to the previously reported from experimental results (Jackson et al. 2016). Secondly, we studied a ZnS/CIGS solar cell and compared it to a CdS/CIGS solar cell. Finally, we investigated the effects of thickness, donor and acceptor densities of the buffer and the absorber layer and the CBO at the ZnS/CIGS interface on the photovoltaic cell parameters in order to improve the photovoltaic CIGS cell performances. The proposed solar cell structure based on ZnS/CIGS showed a conversion efficiency up to 27.33%.

2 Numerical simulation

As our starting point, an initial solar cell structure by using the experimental CIGS solar cell proposed by Jackson et al. (2016) was implemented in this study in the Silvaco-Atlas environment. The simulated cell structure is shown in Fig. 1, which consists of a p–n heterojunction formed by an n-type CdS buffer layer (30 nm) on a p-type CIGS absorber layer (3 μm) with donor and acceptor densities of 3×10^{17} cm^{-3} and 8×10^{16} cm^{-3} respectively. ZnO layer (50 nm) which is a transparent conducting oxide (TCO) used as the front cathode contact and metallic Mo layer (500 nm) represents the back anode contact. The solar cell was considered illuminated under standard conditions for AM 1.5 global solar spectrum (100 mW cm^{-2}) normally incident on the top surface of the ZnO layer.

Simulations were performed using the simulator Atlas-Silvaco that is based on the solution of a set of basic semiconductor equations consisting of the Poisson equation and the continuity and transport equations for free charge carriers (Atlas User's Manual device simulation software 2013). Further, it offers several advanced physical models, which describe the operation of specific electronic devices and material opto-electronic properties. To calculate the performance of the cell structure, it is necessary to specify the electrical parameters of each semiconductor material used in the cell structure. The most parameters of ZnO, CdS and CIGS materials are reported in the literature (Gloeckler et al. 2003; Elbar et al. 2015; Asaduzzaman et al. 2017a, b), or in some cases reasonable estimations are listed in Table 1. The appropriate band gap of CIGS material can be achieved by adjusting gallium content in the absorber layer. Gallium content of the absorber layer is about 0.3 corresponding to a band gap energy of 1.25 eV (Faraj et al. 2011).

Atlas-Silvaco simulations use an input optical files containing the wavelength-dependent refractive index $n (\lambda)$ and extinction coefficient $k (\lambda)$ for the different materials. $n (\lambda)$

Fig. 1 Schematic of CdS/CIGS solar cell

Table 1 Material parameters used in the simulation

Material parameters	ZnO	CdS	ZnS	CIGS
Thickness (µm)	0.05	0.03	0.03	3
Band gap, E_g (eV)	3.3	2.42	3.68	1.25
CB effective density of states, N_C (cm^{-3})	2.2×10^{18}	2.2×10^{18}	1.5×10^{18}	2.2×10^{18}
VB effective density of states, N_V (cm^{-3})	1.8×10^{19}	1.8×10^{19}	1.8×10^{19}	1.8×10^{19}
Electron mobility, μ_n (cm^2 V^{-1} s^{-1})	100	100	250	100
Hole mobility, μ_p (cm^2 V^{-1} s^{-1})	25	25	40	25
Dielectric permitivity, ε	9	10	8.32	13.6
Electron affinity, χ_e (eV)	4.7	4.5	4.5	4.8

and $k(\lambda)$ of Mo, CdS and CIGS materials are available in the Atlas software, while those of ZnO are obtained from (Richter et al. 2013). As CIGS solar cells are known to be susceptible to many unexpected issues during fabrication (such as irregular crystal structure, point defects and high surface roughness), each having the potential to severely deteriorate the cell efficiency. Our simulations considered the combined effects of front surface, back surface, interface states as well as deep-level bulk defects within the absorber and the buffer layers. Shockley–Read–Hall recombination model related to deep defects is considered: acceptor defect density with a Gaussian distribution in the CdS layer (Gloeckler et al. 2003) and donor defect densities with Gaussian distributions in ZnO and CIGS layers (Gloeckler et al. 2003; Song et al. 2010). The density of states is characterized by the effective density of states N_{GA} or N_{GD}, the standard energy deviation W_{GA} or W_{GD}, and the peak energy position E_{GA} or E_{GD}. the subscripts (G, A, D) stand for Gaussian, acceptor and donor defect states, respectively. σ_n and σ_p are the electron and hole capture cross sections of defects. The recombination model at the CdS/CIGS interface and at the front and back contacts is represented by the surface recombination velocities of both electrons (S_n) and holes (S_p) chosen similar and equal to 10^5 cm s^{-1}. The defect parameters are summarized in Table 2 (Gloeckler et al. 2003; Elbar et al. 2015).

3 Results and discussion

3.1 Simulation results of CdS/CIGS solar cell

The energy-band diagram of the ZnO/CdS/CIGS heterostructure is simulated under AM 1.5G illumination and short-circuit conditions using the materials parameters

Table 2 Parameters of gaussian defect states densities used in the simulation

Defect parameters	ZnO	CdS (ZnS)	CIGS
N_{DG}, N_{AG} (cm^{-3})	D: 10^{17}	A: 10^{15}	D: 10^{15}
E_A, E_D (eV)	Midgap	Midgap	Midgap
W_G (eV)	0.1	0.1	0.1
σ_n (cm^2)	10^{-12}	10^{-17}	2×10^{-16}
σ_p (cm^2)	10^{-15}	10^{-13}	2×10^{-15}

summarized in Tables 1 and 2. Figure 2 shows the conduction and valence band energies E_c and E_v of the CIGS absorber, the CdS buffer and the ZnO window. The conduction band offset (CBO) is defined as the difference between the conduction band E_c (the electron affinity) in the buffer layer and the conduction band E_c (the electron affinity) in the absorber at the interface. The energy-band diagram focuses on the heterojunction and does not illustrate the interface CIGS/Mo at the back side of the solar cell. The semiconductor heterojunctions present band discontinuities caused by the difference in band gaps of the semiconductors. Under illumination, if the solar cell is illuminated with photons with energies larger than the band gap energy, electron–hole pairs will be generated in the CIGS absorber. The photogenerated electrons will diffuse into the depleted space-charge region. In the space-charge region the electric field due to the heterojunction is high, the conduction and valence bands are bent, and the photogenerated electrons drift towards the ZnO layer, whereas the photogenerated holes are collected at the Mo contact. Depending on the acceptor and donor densities of the absorber and buffer layers the width of the space-charge region varies. Due to the redistribution of the free charge carriers, the Fermi energy splits into the quasi-Fermi levels E_{Fn} and E_{Fp} for electrons and holes. Depending on the bandgap energy, the CBO can be positive or negative. The CBO between the CdS buffer and the CIGS absorber is positive and the CBO between the ZnO window and the CdS buffer is negative.

The simulated photocurrent–voltage (*I–V*) and the power density–voltage (*P–V*) characteristics of the CdS/CIGS solar cells are shown in Fig. 3. The simulated results were found to deliver a short-circuit current density $J_{sc} = 34.3$ mA cm^{-2}, an open-circuit voltage $V_{oc} = 803$ mV, a fill factor $FF = 82.08\%$ and a conversion efficiency $\eta = 22.6\%$. The achieved conversion efficiency η of 22.6% is in good agreement with literature experimental results (Jackson et al. 2016), thus validating the models and parameters chosen for the simulation.

3.2 Simulation results of ZnS/CIGS solar cell

The ZnS/CIGS solar cell considered has the same CdS/CIGS solar cell structure where the CdS layer was substituted by the ZnS layer with a 0.03 μm thickness and a donor density of 3×10^{17} cm^{-3}. Figure 4 shows the structure of the ZnS/CIGS solar cell.

Fig. 2 Energy-band diagram of the ZnO/CdS/CIGS heterojunction under AM 1.5 illumination and short-circuit conditions
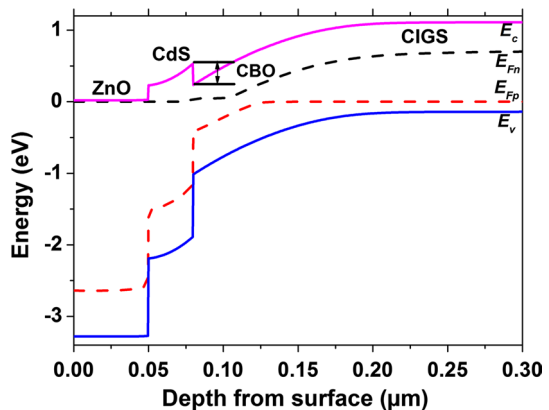
Fig. 3 Simulated I (V) and P (V) characteristics of CdS/CIGS solar cell
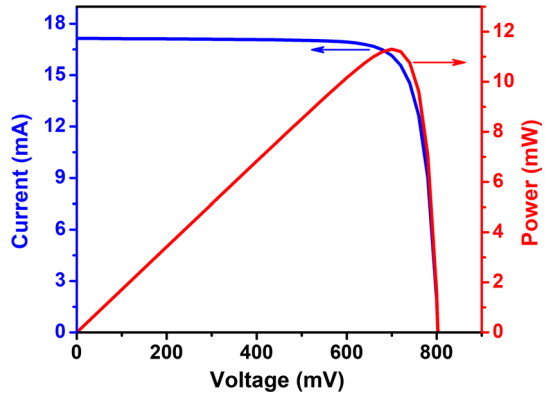

Fig. 4 Schematic of ZnS/CIGS solar cell

Front contact ZnO	(0.05 µm)
Buffer layer n-ZnS 3×10^{17} cm^{-3}	(0.03 µm)
Absorber layer p-CIGS 8×10^{16} cm^{-3}	(3 µm)
Back contact Mo	(0.5 µm)

The simulation parameters of the ZnS material are based on the literature (Haque et al. 2014; Singh et al. 2016) and are displayed in Tables 1 and 2. Refractive index n (λ) and extinction coefficient k (λ) for ZnS layer are available in the Atlas software. A deep acceptor defect density with a Gaussian distribution in the ZnS layer was considered (Pettersson et al. 2013). Figure 5 shows the simulated I–V and P–V characteristics of the ZnS/CIGS solar cell.

A comparison of the photovoltaic parameters of CdS/CIGS and ZnS/CIGS solar cells is given in Table 3. The short-circuit current density J_{sc} of the ZnS/CIGS cell is higher than that of the CdS/CIGS cell because the absorption of light for short wavelengths by the ZnS material is low. This is clearly seen in Fig. 6 where the optical absorption coefficient of ZnS material is lower compared to CdS material in the range of 350–1000 nm. The external quantum efficiency (EQE) as a function of wavelength for the ZnS/CIGS cell is shown in Fig. 7. The enhanced absorption of the ZnS/CIGS solar cell in the short wavelength region between 300 and 450 nm compared with the CdS/CIGS solar cell leads to an improved quantum efficiency with a gain in short-circuit current density J_{sc} of 1.36 mA cm^{-12}. On the other hand, the open circuit voltage V_{oc} of the ZnS/CIGS cell is almost the same as that of the CdS/CIGS cell. The fill factor of the ZnS/CIGS solar cell is slightly higher than that of the CdS/CIGS solar cell. The highest conversion efficiency of 23.54% is obtained for the ZnS/CIGS solar cell compared with the conversion efficiency of 22.6% for the CdS/CIGS

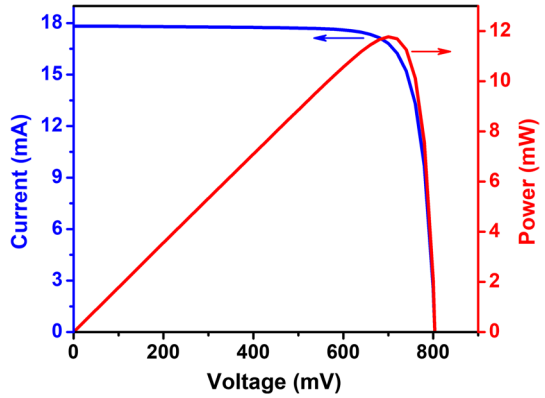**Fig. 5** Simulation *I–V* and *P–V* characteristics of the ZnS/CIGS solar cell

Table 3 Photovoltaic parameters of CdS/CIGS and ZnS/CIGS solar cells

Structures	J_{sc} (mA cm^{-2})	V_{oc} (V)	*FF* (%)	η (%)
CdS/CIGS cell	34.30	0.803	82.08	22.60
ZnS/CIGS cell	35.66	0.804	82.14	23.54

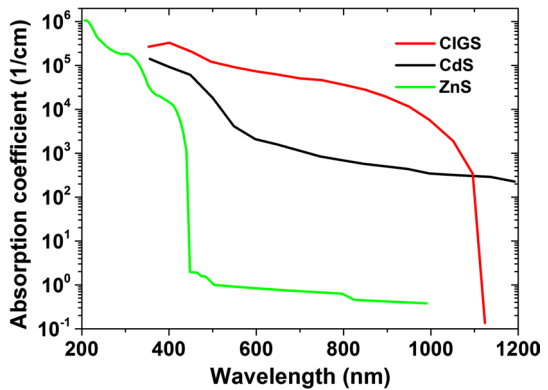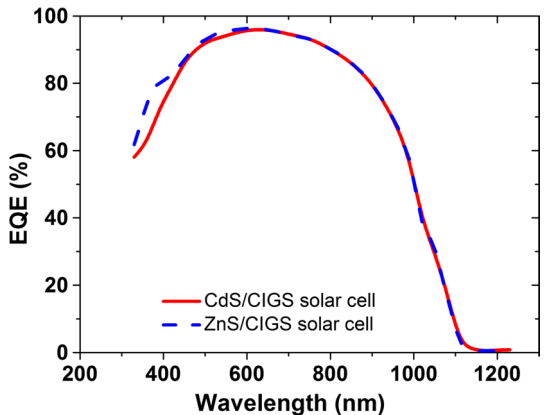**Fig. 6** Wavelength-dependant absorption coefficients of CIGS, CdS and ZnS semiconductor materials

Fig. 7 Simulated external quantum efficiency of the best ZnS/CIGS solar cell as compared with a CdS/CIGS solar cell

solar cell, due to increased J_{sc} and *FF*. This results ensure the suitability of ZnS buffer layer in CIGS solar cells.

In the following, we will study the effects of certain properties of ZnS and CIGS layers mainly, thickness, donor and acceptor densities and CBO at interface ZnS/CIGS layers on the performance of the ZnS/CIGS solar cell.

3.3 Effects of donor and acceptor densities of ZnS and CIGS layers

We varied the ZnS and CIGS donor and acceptor densities from 10^{15} to 10^{18} cm^{-3} with the thicknesses of the ZnS and CIGS layers being fixed at 30 nm and 3 μm respectively. The results are shown in Fig. 8. When the acceptor density of the CIGS absorber layer increases from 10^{15} to 10^{18} cm^{-3}, there is a decrease in the short circuit current density J_{sc} from 37.45 to 34.63 mA cm^{-2} but there is a small effect of the donor density variation of the ZnS buffer layer on the short-circuit current density J_{sc}. On the other hand, the open-circuit voltage V_{oc} increases from 682 to 882 mV when the acceptor density of the CIGS layer increases from 10^{15} to 10^{18} cm^{-3} while the donor density effect of the ZnS layer on the open-circuit voltage V_{oc} is low. We also noticed a rapid increase in the conversion efficiency η for acceptor and donor densities of the CIGS and ZnS layers between 2×10^{17} and 10^{18} cm^{-3} caused by the improvement of the fill factor
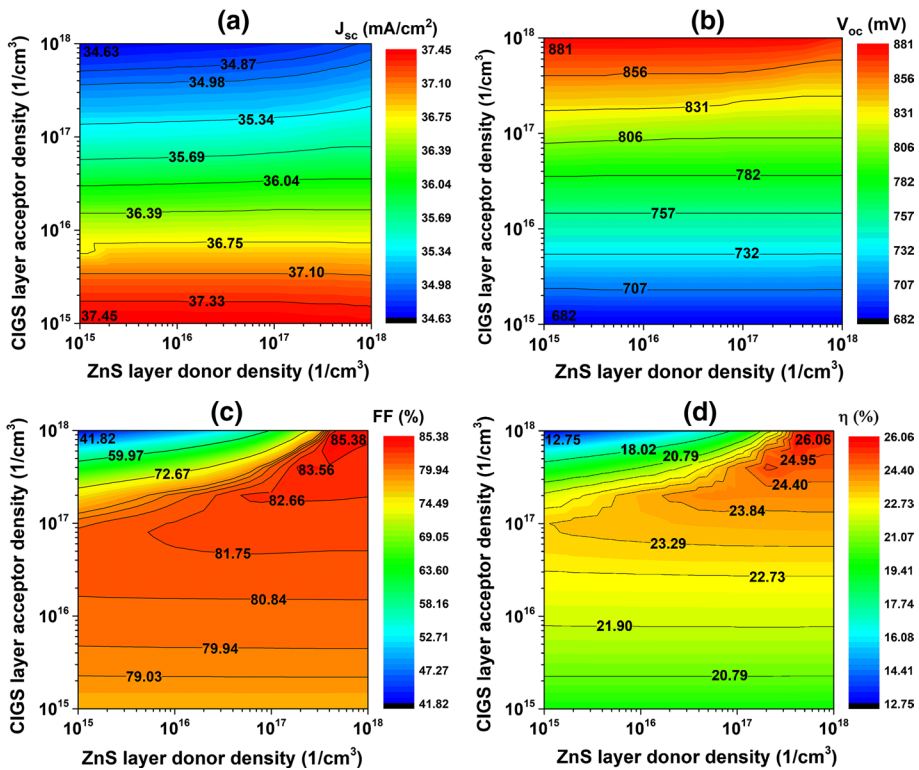

Fig. 8 Photovoltaic parameters as function of ZnS and CIGS donor and acceptor densities of a ZnS/CIGS solar cell: **a** short-circuit current density (J_{sc}), **b** open-circuit voltage (V_{oc}), **c** fill factor (*FF*) and **d** conversion efficiency (η)

with the increase of acceptor and donor densities of the CIGS and ZnS layers between 2×10^{17} and 10^{18} cm^{-3} and the improvement of the open circuit voltage with increasing the CIGS acceptor density. The electric field increases also with the donor and acceptor densities of the ZnS/CIGS heterojunction which improves the collection of the photogenerated carriers and therefore enhances the conversion efficiency. A higher acceptor density of the CIGS absorber layer, on the other hand, brings impact on electric field build-up within the space charge region. A higher electric field reduces the free carrier recombination which basically increases the V_{oc}. However, a higher value of the acceptor density of the CIGS absorber layer correspond to an increase in the carrier recombination in the bulk, which thus reduces the magnitude of the short-circuit current density. The increase of the conversion efficiency is mainly due to the increase of the open-circuit voltage V_{oc} and the fill factor FF. The highest conversion efficiency of 26.06% is obtained at donor and acceptor densities of the ZnS and CIGS layers of 6×10^{17} cm^{-3} and 1×10^{18} cm^{-3}, respectively. The addition of Ga makes the CIGS material p-type. Therefore, by varying the Ga content, the acceptor concentration can be optimized in principle, although challenging. To dope the ZnS material, elements of group III or group VII will increase the electrical conductivity of the films. However, the doping which consists in adding of some of these elements may disrupt the crystallinity, increasing the number of defects, and reducing the required electrical conductivity. The optimum electrical conductivity is a challenging task to obtain, but every positive step will contribute to the enhancement of the cell performance.

3.4 Effects of thicknesses of ZnS and CIGS layers

The thickness of the ZnS layer is varied from 10 to 50 nm while the thickness of the CIGS layer is varied from 1 to 4 µm. The donor and acceptor densities of ZnS and CIGS layers were fixed to 6×10^{17} cm^{-3} and 1×10^{18} cm^{-3}, respectively. The effects of the thicknesses of the ZnS and CIGS layers on the photovoltaic parameters of the ZnS/CIGS solar cell are illustrated in Fig. 9. The short-circuit current density increases from 30.69 to 35.70 mA cm^{-12} with the increase of the CIGS absorber layer thickness from 1 to 4 µm and the ZnS buffer layer thickness between 10 and 35 nm. The open-circuit voltage V_{oc} increases also and attains a maximum value of 0.882 V for the ZnS buffer layer thickness of 0.03 µm and the CIGS absorber layer thickness of 4 µm. The increase of J_{sc} and V_{oc} result in increasing the conversion efficiency of the solar cell. A very thin absorbing layer means that the back contact and the depletion region are very close, which promotes the capture of electrons by the back contact. This form of recombination process is detrimental to the cell performance as it affects J_{sc}, V_{oc} and η of the solar cell. The increase of the ZnS buffer layer thickness from 35 to 50 nm leads to a decrease of all the cell parameters. When the thickness of the ZnS layer increases, more photons are absorbed by the ZnS layer and few photons reach the CIGS absorbing layer which leads to the drop of the photocurrent. The highest conversion efficiency of 26.82% is obtained with ZnS and CIGS layer thicknesses of 25 nm and 4 µm, respectively.
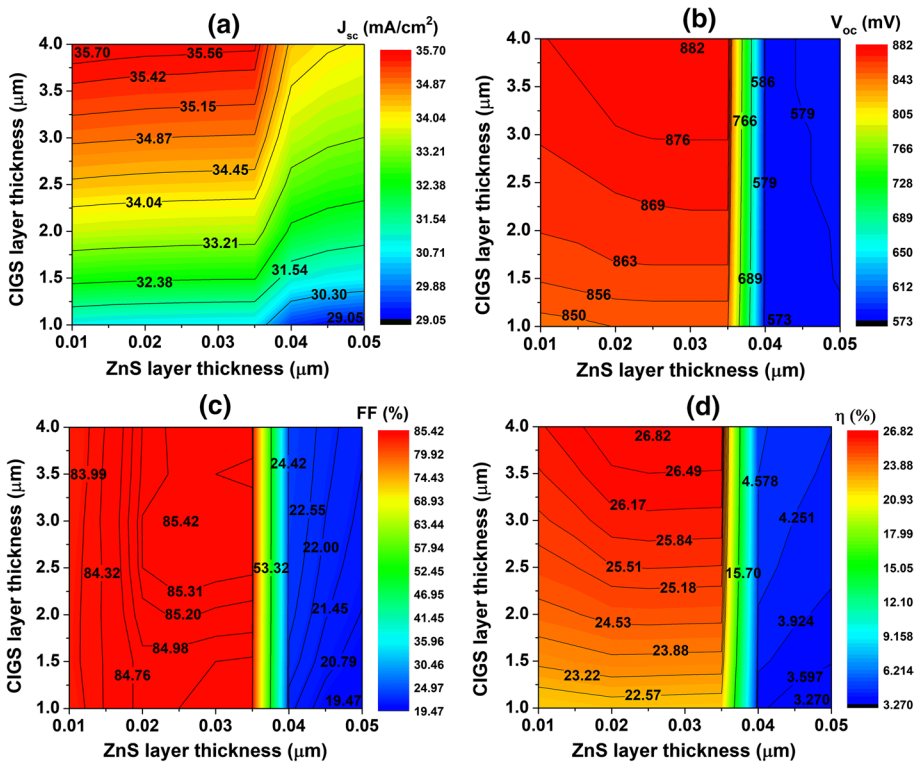
Fig. 9 Photovoltaic parameters as function of ZnS and CIGS thicknesses of a ZnS/CIGS solar cell: **a** short-circuit current density (J_{sc}), **b** open-circuit voltage (V_{oc}), **c** fill factor (*FF*) and **d** conversion efficiency (η)

3.5 Effect of conduction band offset at interface ZnS/CIGS layers

The Conduction Band Offset (CBO) which represents the electron affinity difference between the ZnS buffer layer and the CIGS absorber layer was investigated in this numerical simulation. The band gap of the ZnS buffer layer was assumed a constant of 3.68 eV and the CBO was varied by changing the electron affinity of ZnS layer from 4.15 to 5.8 eV with the CIGS electron affinity assumed constant at 4.8 eV. The effects of the CBO on the photovoltaic parameters of the ZnS/CIGS solar cell are illustrated in Fig. 10. A positive CBO indicates that a conduction band of the ZnS buffer layer is above that of the CIGS absorber layer. Conversely, a negative CBO indicates that a conduction band of the ZnS buffer layer is below that of the CIGS absorber layer. The CBO was varied from − 1 to 0.65 eV. The short-circuit current density is constant in the range of the CBO from − 1 to 0.55 eV. When the conduction band of window layer is below that of CIGS, the barrier against photogenerated electrons is not formed and the short-circuit current is nearly constant. Over the CBO value of 0.55 eV, the short-circuit current decreases abruptly. In this region, the conduction band of the ZnS buffer layer is above that of the CIGS absorber layer, the barrier against photogenerated electrons is formed and the short–circuit current decreases abruptly. This result is in good agreement with the previous results reported in Ramli et al. (2013) and
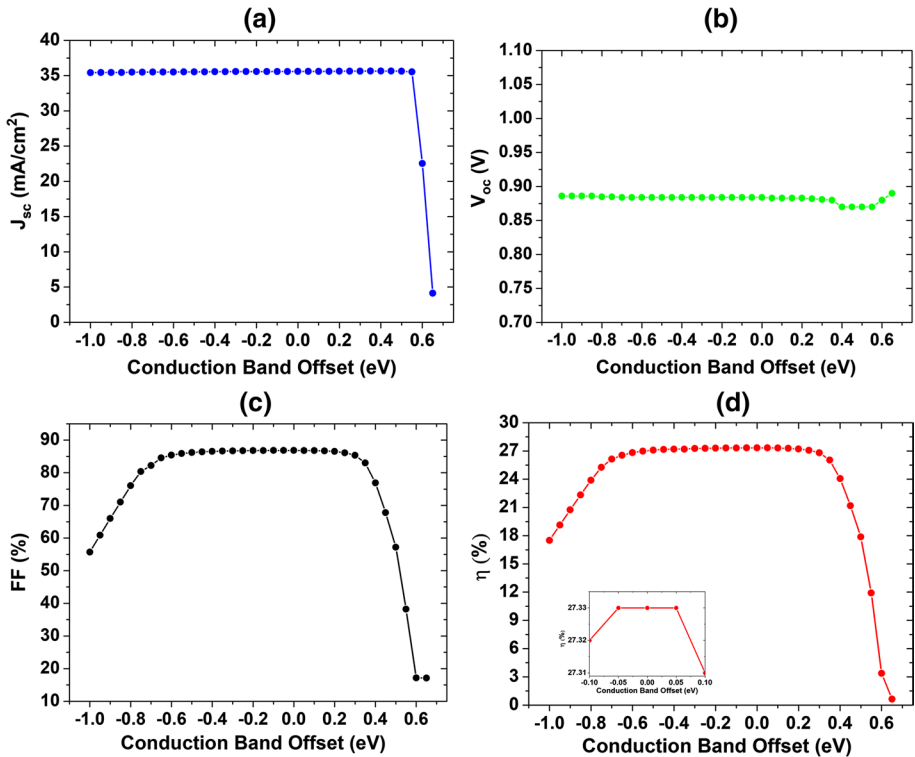
Fig. 10 Photovoltaic parameters as function of Conduction Band Offset of a ZnS/CIGS solar cell: **a** short-circuit current density (J_{sc}), **b** open-circuit voltage (V_{oc}), **c** fill factor (*FF*) and **d** conversion efficiency (η)

Bechlaghem et al. (2018). The open-circuit voltage is nearly constant. The same as the short-circuit current, the fill factor increases in the CBO range of − 1 to 0.65 eV. The fill factor is nearly constant as the CBO is in the range of − 0.65 to 0.35 eV and over 0.35 eV the fill factor decreases abruptly. In this region, the conduction band of the ZnS buffer layer is above that of the CIGS absorber layer, the barrier against photogenerated electrons is formed and the fill factor decreases abruptly due to the short-circuit current decrease abruptly. This results are confirmed with simulation results reported in Bechlaghem et al. (2018) and Sozzi et al. (2014). When the CBO is in the range of − 0.65 to 0.25 eV, an excellent performance is obtained with a high conversion efficiency of 27.33% achieved at the CBO in the range of − 0.05 to 0.05 eV. This result can be attributed to the favourable band alignment at the ZnS/CIGS interface. Therefore, adjusting the CBO of the ZnS/CIGS interface is necessary to improve the performance of the ZnS/CIGS solar cells.

At the end of this analysis, the results obtained for our optimized solar cell are better than those obtained in recent work by Fridolin et al. (2018); they simulated a ZnS/CIGS solar cell by using the software SCAPS and obtained a high efficiency of 26.3% after optimizing the materials properties such as the electron affinity and the thickness of the ZnS layer, the acceptor density and the thickness of the CIGS layer.

4 Conclusion

In the present work, we studied numerically a CIGS based thin-film solar cell by using the device simulator Silvaco-Atlas. Firstly, we simulated a standard solar cell of CdS/CIGS and the simulation results are in agreement with experimental results found in literature. Secondly, we studied a ZnS/CIGS solar cell and the simulation results prove that the cell with the ZnS buffer layer is better with respect to the standard solar cell cell of CdS/CIGS. Finally, we investigated the effects of the thicknesses, the donor and acceptor densities of ZnS and CIGS layers and the CBO at ZnS/CIGS interface on the photovoltaic cell parameters. As a result, the maximum efficiency of 27.33% was obtained for the ZnS buffer layer and CIGS absorber layer thicknesses of 0.025 and 4 μm doped with 6×10^{17} and 10^{18} cm^{-3} respectively and the CBO at interface ZnS/CIGS layers in the range -0.05 to 0.05 eV. These simulation results indicate that the ZnS material properties are promising and can improve the CIGS based thin-film solar cell efficiency. The ZnS material also plays an important role for overcoming the serious environmental related problems due to the toxic nature of cadmium. The present results of simulation may benefit the development of the solar cells with higher conversion efficiency and low cost.

References

Asaduzzaman, Md., Bahar, A.N., Bhuiyan, M.M.R.: Dataset demonstrating the modeling of a high performance Cu(In, Ga)Se$_2$ absorber based thin film photovoltaic cell. Data Brief **11**, 296–300 (2017a)

Asaduzzaman, Md, Billal Hosen, Md, Karamot Ali, Md, Newaz Bahar, A.: Non-toxic buffer layers in flexible Cu(In, Ga)Se$_2$ photovoltaic cell applications with optimized absorber thickness. Int. J. Photoener. **2017**, 187–191 (2017b)

Atlas User's Manual device simulation software. Silvaco, Inc, Santa Clara, USA (2013)

Bechlaghem, S., Zebentout, B., Benamara, Z.: The major influence of the conduction-band-offset on Zn(O, S)/CuIn$_{0.7}$Ga$_{0.3}$Se$_2$ solar cells. Results. Phys. **10**, 650–654 (2018)

Chelvanathan, P., Hossain, M.I., Amin, N.: Performance analysis of copper–indium–gallium–diselenide (CIGS) solar cells with various buffer layers by SCAPS. Curr. Appl. Phys. **10**(3), S387–S391 (2010)

Elbar, M., Tobbeche, S., Merazga, A.: Effect of top-cell CGS thickness on the performance of CGS/CIGS tandem solar cell. J. Sol. Energy. **125**, 104–112 (2015)

Faraj, M.G., Ibrahim, K., Salhin, A.: Investigation of CIGS solar cells on polyethylene terephthalate substrates. Int. J. Polym. Mater. **60**(10), 817–824 (2011)

Fridolin, T.N., Maurel, D.K.G., Ejuh, G.W., Bénédicte, T.T., Marie, N.J.: Highlighting some layer's properties in performances optimization of CIGSe based solar cells: case of Cu (In, Ga) Se–ZnS. J. King Saud Univ. Sci. (2018). https://doi.org/10.1016/j.jksus.2018.03.026

Friedlmeier, T.M., Jackson, P., Bauer, A., Hariskos, D., Kiowski, O., Wuerz, R., Powalla, M.: Improved photocurrent in Cu(In, Ga)Se$_2$ solar cells: from 20.8% to 21.7% efficiency with CdS buffer and 21.0% Cd-free. J. Photovolt. **5**, 1487–1491 (2015)

Gloeckler, M., Fahrenbruch, A.L., Sites, J.R.: Numerical modeling of CIGS and CdTe solar cells: setting the baseline. In: 3rd World Conference on Photovoltaic Energy Conversion, pp. 491–494 (2003)

Haque, F., Khan, N.A., Rahman, K.S., Islam, M.A., Alam, M.M., Sopian, K., Amin, N.: Prospects of zinc sulphide as an alternative buffer layer for CZTS solar cells from numerical analysis. In: 8th International Conference on Electrical and Computer Engineering, pp. 504–507 (2014)

Hariskos, D., Spiering, S., Powalla, M.: Buffer layers in Cu(In, Ga)Se$_2$ solar cells and modules. Thin Solid Films **480**, 99–109 (2005)

Hosen, M.B., Bahar, A.N., Ali, M.K., Asaduzzaman, M.: Modeling and performance analysis dataset of a CIGS solar cell with ZnS buffer layer. Data Brief **14**, 246–250 (2017)

Jackson, P., Wuerz, R., Hariskos, D., Lotter, E., Witte, W., Powalla, M.: Effects of heavy alkali elements in Cu(In, Ga)Se$_2$ solar cells with efficiencies up to 22.6%. Phys. Status Solidi RRL **10**, 583–586 (2016)

Khoshsirat, N., Yunus, N.A.M., Hamidon, M.N., Shafie, S., Amin, N.: Analysis of absorber layer properties effect on CIGS solar cell performance using SCAPS. Optik **126**, 681–686 (2015)

Lindahl, J., Zimmermann, U., Szaniawski, P., Torndahl, T., Hultqvist, A., Salome, P., Platzer-Bjorkman, C., Edoff, M.: Inline Cu(In, Ga)Se$_2$ Co-evaporation for high-efficiency solar cells and modules. IEEE. J. Photovolt. **3**, 1100–1105 (2013)

Luo, K., Sun, Y., Zhou, L., Wang, F., Wu, F.: Theoretical simulation of performances in CIGS thin-film solar cells with cadmium-free buffer layer. J. Semicond. **38**(8), 084006 (2017)

Martin Green, A., Emery, K., Hishikawa, Y., Warta, W., Ewan Dunlop, D., Dean Levi, H., Anita Ho-Baillie, W.Y.: Solar cell efficiency tables (Version 49). Prog. Photovolt.: Res. Appl. **25**, 23–32 (2016)

Mostefaoui, M., Mazari, H., Khelifi, S., Bouraiou, A., Dabou, R.: Simulation of high efficiency CIGS solar cells with SCAPS-1D software. Energy Procedia **74**, 736–744 (2015)

Movla, H.: Optimization of the CIGS based thin film solar cells: numerical simulation and analysis. Optik **125**(1), 67–70 (2014)

Nakamura, M, Yamaguchi, K, Chiba, Y, Hakuma, H, Kobayashi, T, Nakada, T.: Achievement of 19.7% efficiency, with a small-sized Cu(In,Ga)(Se,S)$_2$ solar cells prepared by sulfurization after selenization process with Zn-based buffer. In: 39th IEEE Photovoltaic Specialists Conference, pp. 0849–0852 (2013)

Park, J., Shin, M.: Numerical optimization of gradient bandgap structure for CIGS solar cell with ZnS buffer layer using technology computer-aided design simulation. Energies **11**(7), 1785–1794 (2018)

Pettersson, J., Törndahl, T., Platzer-Björkman, C., Hultqvist, A., Edoff, M.: The influence of absorber thickness on Cu(In, Ga)Se solar cells with different buffer layers. IEEE. J. Photovolt. **3**, 1376–1382 (2013)

Ramli, H., Rahim, S.K.A., Rahim, T.A., Aminuddin, M.M.: Optimization of zinc sulfide (ZnS) electron affinity in copper indium sulfide (CIS) based photovoltaic cell. Chal. Lett. **10**(6), 189–195 (2013)

Richter, M., Schubert, C., Eraerds, P., Riedel, I., Keller, J., Parisi, J., Dalibor, T., Avellán-Hampe, A.: Optical characterization and modeling of Cu(In, Ga)(Se, S)$_2$ solar cells with spectroscopic ellipsometry and coherent numerical simulation. Thin Solid Films **535**, 331–335 (2013)

Siebentritt, S.: Alternative buffers for chalcopyrite solar cells. Sol. Energy **77**, 767–775 (2004)

Singh, P., Gautam, R., Sharma, S., Kumari, S., Verma, A.S.: Simulated solar cell device of CuGaSe$_2$ by using CdS, ZnS and ZnSe buffer layers. Mater. Sci. Semicond. Process. **42**, 288–302 (2016)

Song, S.H., Nagaich, K., Aydil, E.S., Feist, R., Haley, R., Campbell, S.A.: Structure optimization for a high efficiency CIGS solar cell. In: 35th IEEE Photovoltaic Specialists Conference, pp. 2488–2492 (2010)

Sozzi, G., Troni, F., Menozzi, R.: On the combined effects of window/buffer and buffer/absorber conduction-band offsets, buffer thickness and doping on thin-film solar cell performance. Sol. Energy. Mater. Solar Cell. **121**, 126–136 (2014)

Spiering, S., Nowitzki, A., Kessler, F., Igalson, M., Maksoud, H.A.: Optimization of buffer-window layer system for CIGS thin film devices with indium sulphide buffer by in-line evaporation. Sol. Energy. Mater. Sol. Cell. **144**, 544–550 (2016)

Sylla, A., Touré, S., Vilcot, J.P.: Theoretical analysis of the effects of band gaps and the conduction band offset of ZnS-CIGS layers, as well as defect layer thickness. Int. J. Sci. Res. **6**(11), 855–861. https://www.ijsr.net/archive/v6i11/v6i11.php. #ijsrnet (2017)

Törndahl, T., Hultqvist, A., Platzer-Björkman, C., Edoff, M.: Growth and characterization of ZnO-based buffer layers for CIGS solar cells. In: Oxide-Based Materials and Devices, vol. 7603, p. 76030D (2010)

Za'Abar, F., Zuhdi, A.W.M., Bahrudin, M.S., Abdullah, S.F., Harif, M.N., Hasani, A.H.: Optimization of baseline parameters and numerical simulation for Cu (In, Ga)Se$_2$ solar cell. In: IEEE International Conference on Semiconductor Electronics (ICSE), pp. 209–213 (2018)

Springer